

An Empirical Model for Dual-Diversity Reception over Fixed Wireless Channels in Suburban Macrocell Environments

David G. Michelson, *Senior Member, IEEE*, Vinko Erceg, *Fellow, IEEE*,
Saeed S. Ghassemzadeh, *Senior Member, IEEE*, and Larry J. Greenstein, *Life Fellow, IEEE*

Abstract—Fixed wireless multipoint communication systems are increasingly being deployed in suburban macrocell environments, either to provide voice and data services to residences (wideband systems) or to supply automated meter reading and related supervisory control and data acquisition services (narrowband systems). Here, we show that a particularly simple yet complete first-order statistical characterization of two-branch diversity reception over fixed wireless channels can be given in terms of just five channel parameters: the average path gains and Ricean K-factors for each branch and the complex envelope correlation coefficient between the time-varying parts of the two path gains. We further show that all five parameters can be estimated from amplitude-only measurements of path gain vs. time, subject only to the assumption that the time-varying component of the path gain is complex Gaussian. We present representative sets of model parameters based upon data collected in typical suburban macrocell environments over time, location, and/or frequency using polarization diversity antennas. Because each of the model parameters, or its logarithm, is close to Gaussian, the set may be cast as a five-element vector of jointly random Gaussian processes. Despite obvious physical differences between the environments, the results show a remarkable consistency.

Index Terms—Antenna diversity, channel model, fading channel, fixed wireless channel.

I. INTRODUCTION

INTEREST in non-line-of-sight (NLOS) fixed wireless channels in suburban macrocell environments has developed in two distinct phases during the past decade. In the first phase, interest was focused on fixed wireless multipoint communication systems (MCS) that operate in the high UHF bands and above and which are used by telecommunications service providers to deliver broadband voice and data services to suburban households. In the second phase, which

is just beginning, interest is expanding to include emerging narrowband multipoint communication systems (N-MCS) that will operate in both VHF and UHF bands and be used by utility companies for automated meter reading and similar supervisory control and data acquisition (SCADA) services. Compared to conventional MCSs, N-MCSs support much lower data rates but the expectations for their reliability are often much greater.

Simulations of communication systems that use diversity reception to mitigate fading over narrowband fixed wireless channels require a statistical characterization of the relevant channel parameters. At the system level, a broadband path loss model and information concerning the cell size, the number and distribution of users, and the base station and remote terminal antenna patterns can be used to estimate the levels of signal and interference experienced by each user. At the channel level, these parameters can be combined with a narrowband dual-branch channel model to yield estimates of the time-varying path gains, $g_1(t)$ and $g_2(t)$, and signal-to-interference-and-noise ratios for each user. If, as in the case of most fixed wireless communication systems, the fading rate is much slower than the symbol rate, the first-order statistics of path gain, combined with knowledge of the modulation, coding, and diversity schemes, are sufficient to model the capacities and outage probabilities of the links within such systems.

Measurement-based statistical models of fixed wireless channels are of particular interest because they provide insight concerning the behavior of channel parameters which are difficult to model by deterministic means [1]–[4]. In previous work, we revealed that a complete first-order statistical characterization of two-branch diversity reception over narrowband fixed wireless channels can be given in terms of just five channel parameters: the average path gains and Ricean K-factors for each branch and the complex envelope correlation coefficient between the time-varying parts of the two path gains [5],[6]. Moreover, we noted that preliminary measurements that we collected in typical suburban environments suggest that each of these parameters, or its logarithm, is close to Gaussian. This implies that the set may be cast as a five-element vector of jointly Gaussian variates that are completely specified by the means, standard deviations and mutual correlation coefficients of the five parameters.

Although this previous work revealed some general trends,

Manuscript received June 28, 2008; revised March 31, 2009; accepted April 2, 2009. The associate editor coordinating the review of this paper and approving it for publication was R. Murch.

D. G. Michelson is with the Radio Science Laboratory, Department of Electrical and Computer Engineering, University of British Columbia, Vancouver, BC, Canada V6T 1Z4 (e-mail: davem@ece.ubc.ca).

V. Erceg is with the Broadcom Corporation, San Diego, CA 92128 USA (e-mail: verceg@broadcom.com).

S. S. Ghassemzadeh is with the Communications Technology Research Department, AT&T Labs - Research, Florham Park, NJ 07932 USA (e-mail: saeedg@research.att.com).

L. J. Greenstein is with the Wireless Information Network Laboratory, Rutgers University, North Brunswick, NJ 08902 USA (e-mail: ljg@winlab.rutgers.edu).

Digital Object Identifier 10.1109/TWC.2009.080853

designers need to know: (1) the actual first-order model parameters that one can apply in typical suburban macrocell environments, (2) how the model parameters differ when the service areas have different terrain morphologies or foliage densities, and (3) what patterns or symmetries exist in the correlation matrix that relates the first-order model parameters. Here, we present the results of a series of measurement campaigns that we conducted in and around typical suburban environments with flat and rolling terrain and light-to-heavy foliage densities in an effort to resolve these issues. Because a base station generally serves remote terminals at many different locations throughout its coverage area using different channels within an assigned sub-band, we base our numerical results on data collected over time, location, and, in certain cases, multiple frequencies.

The remainder of this paper is organized as follows: In Section II, we review the essential aspects of our first-order description of the dual diversity channel response, including the methods that we used to estimate the relevant channel parameters from amplitude-only measurements of narrowband path gain vs. time. In Section III, we describe our collection of such data in representative suburban macrocell environments. In Section IV, we present both our state vector model that summarizes our results and our interpretation of the model parameters. In Section V, we summarize our key findings and their implications.

II. THE MODEL AND ITS PARAMETERS

The complex signal path gain of a narrowband channel (typically tens of kHz wide) over a given time segment (typically several minutes long) is given by

$$g(t) = V + v(t), \quad (1)$$

where V is a complex number and $v(t)$ is a complex, zero-mean random time variation caused by wind-blown foliage, vehicular traffic, etc. Both V and the parameters of the random process $v(t)$ may change from one time segment to another. In many field measurement situations, we are restricted to collecting time series measurements of $|g(t)|^2$, i.e., power only, no phase information. We can estimate the statistical parameters of such time series as follows.

A. Average Gain and Ricean K -factor

From time series data collected over a given time segment (several minutes in length), we can calculate the average power gain,

$$G = \overline{|g(t)|^2}, \quad (2)$$

which, in terms of (1), is given by

$$G = |V|^2 + \overline{|v(t)|^2} = |V|^2 + \sigma^2. \quad (3)$$

where σ^2 is the power in the time-varying component. The rms fluctuation of the envelope about the mean is given by the standard deviation of $|g(t)|^2$ and is denoted by σ_G . Because experience has shown that $v(t)$ is a complex Gaussian process, the distribution of $|g(t)|$ over time is Ricean with a K -factor given by

$$K = |V|^2 / \overline{|v(t)|^2}. \quad (4)$$

Various methods for estimating K have been proposed; we use the moment-based method described in [8] where

$$K = \frac{|V|^2}{\sigma^2} = \frac{\sqrt{G^2 - \sigma_G^2}}{G - \sqrt{G^2 - \sigma_G^2}}. \quad (5)$$

In a small fraction of cases, σ_G may exceed G , either due to the finite size of the data population (a statistical effect), or because $v(t)$ is not complex Gaussian, as assumed. In either case, eqn. (5) does not give a real solution for K . Our approach in such cases is as follows: If G and σ_G are within a few percent of each other, we assume statistical error and set $K = 0$. Otherwise, we do not process this segment. The percentage of cases which correspond to the second instance is generally very small (typically 1-2%). In terms of G and K , the expression for $g(t)$ in (1) can be re-cast in terms of G and K as

$$g(t) = \sqrt{\frac{G}{K+1}} \left[\sqrt{K} e^{j\psi} + x(t) \right], \quad (6)$$

where ψ is the phase of V and $x(t)$ is a zero-mean complex Gaussian process with unit standard deviation. Because only the relative phase is of interest, expressions for the signal gains $g_1(t)$ and $g_2(t)$ can be given by

$$g_1(t) = \sqrt{\frac{G_1}{K_1+1}} \left[\sqrt{K_1} + x_1(t) \right] \quad (7)$$

and

$$g_2(t) = \sqrt{\frac{G_2}{K_2+1}} \left[\sqrt{K_2} e^{j\Delta\Psi} + x_2(t) \right], \quad (8)$$

where $\Delta\Psi = \Psi_2 - \Psi_1$. The correlation between the complex Gaussian variates x_1 and x_2 is denoted by

$$\rho_{env} = \overline{x_1 x_2^*} = \text{Re} e^{j\theta} \quad (9)$$

where R and θ are the magnitude and phase of ρ_{env} , respectively. From (7) and (8), the channel parameters G_1 , G_2 , K_1 , K_2 , and ρ_{env} completely specify the first-order statistics of the two branch gains over time intervals of several minutes.

B. Complex Envelope Correlation Coefficient

We now show how to estimate the complex envelope correlation coefficient ρ_{env} given knowledge of the correlation coefficient between the power signals $|g_1|^2$ and $|g_2|^2$, i.e.,

$$\rho_{pwr} = \frac{(|g_1|^2 - \mu_{|g_1|^2})(|g_2|^2 - \mu_{|g_2|^2})}{\sigma_{|g_1|^2} \sigma_{|g_2|^2}}. \quad (10)$$

Under the assumption that the time-varying components $v_1(t)$ and $v_2(t)$ are both complex Gaussian, it can be shown using (7) and (8) that

$$\rho_{pwr} = \frac{R^2 + 2\sqrt{K_1 K_2} R \cos \theta}{\sqrt{(2K_1 + 1)(2K_2 + 1)}}, \quad (11)$$

where R and θ are defined by eqn. (9) and ρ_{pwr} , K_1 , and K_2 can be estimated from the measured data. Subject to the obvious constraint that $0 \leq R \leq 1$, there is a continuous locus of points in $R - \theta$ space that satisfies (11). We choose that $R - \theta$ combination that yields a worst-case value for $\text{Re} e^{j\theta}$, i.e., the complex value that would give the poorest performance results in system simulations. It can be reasoned that this

worst-case solution is the one for which $R \cos \theta$, subject to (11), is maximized¹. If $\rho_{pwr} < 0$, this occurs when

$$\begin{aligned} R &= \sqrt{K_1 K_2} - \sqrt{K_1 K_2 + D}, \\ \theta &= \pi \end{aligned} \quad (12)$$

where

$$D = \rho_{pwr} \sqrt{(2K_1 + 1)(2K_2 + 1)}. \quad (13)$$

Otherwise, if $\rho_{pwr} > 0$, $R \cos \theta$ is maximized when

$$\begin{aligned} R &= -\sqrt{K_1 K_2} + \sqrt{K_1 K_2 + D}, \\ \theta &= 0 \end{aligned} \quad (14)$$

Combining the above solutions, we obtain a compact form for $Re^{j\theta}$, i.e.,

$$\rho_{env} = Re^{j\theta} = -\sqrt{K_1 K_2} + \sqrt{K_1 K_2 + D}. \quad (15)$$

Thus, our worst-case estimate of ρ_{env} is real and bipolar. Note, however, that there is no real solution for R if

$$\rho_{env} = \frac{-K_1 K_2}{\sqrt{(2K_1 + 1)(2K_2 + 1)}}, \quad (16)$$

as is clear from (13) and (15). Since negative ρ_{pwr} , implies that $R \cos \theta$ is negative, a conservative bound in this case is just $\rho_{env} = 0$. That is the approach we take here. Throughout our data reductions, we have consistently found that ρ_{env} , computed as above, has much the same probability distribution as ρ_{pwr} , computed directly from the instantaneously received powers. Typical results, based on data collected in the environments with rolling terrain, are shown in Fig. 1. Thus, the distribution of ρ_{pwr} , which is easily obtained from amplitude-only data, reliably predicts a worst-case distribution for ρ_{env} .

III. EXPERIMENTAL RESULTS

A. Data Collections

We conducted a series of measurement campaigns aimed at characterizing fixed wireless propagation in suburban macro-cell environments at 2 GHz. All of the links were obstructed by intervening buildings, foliage or, in some cases, terrain; none could be classified as line-of-sight (LOS). We measured the narrowband path gains of fixed wireless diversity channels, over both time and location, in neighborhoods with flat terrain and light-to-moderate foliage (downlinks in Naperville and Bellwood, IL); two neighborhoods with rolling terrain and moderate-to-heavy foliage (downlinks in Whippany and Iselin, NJ); and one neighborhood with flat terrain and heavy foliage (uplinks in Vancouver, BC). Some of our measurement data were collected using a single carrier transmitter and a single-frequency diversity receiver, while others were collected using a multiple carrier transmitter and a swept frequency diversity receiver. In all cases, the transmit antenna was vertically polarized and the receiving antennas had cross-slant elements (by which we mean two linearly polarized elements that are orthogonal to each other and slanted ± 45 degrees from the vertical. The details are presented in Tables I-III.

¹To see this, note that dual-channel operation works best when $g_1(t)$ and $g_2(t)$ are the most dissimilar, i.e., when the rms value of $|g_1(t) - g_2(t)|$ is greatest, and that this quantity decreases monotonically as $R \cos \theta$ increases from -1 to +1.

1) *The Neighborhoods with Flat Terrain and Light-to-Moderate Foliage:* We collected downlink measurements at randomly selected locations in the vicinity of two cellular base stations in Illinois, one in Naperville and the other in Bellwood. In Naperville, the homes are more openly spaced and the foliage is younger and less dense than in Bellwood. A total of 205.5 hours of data were collected at 35 receive locations. In Naperville, 122 hours of data were collected at 21 receive locations with distances ranging from 0.59 km to 2.11 km. In Bellwood, 83.5 hours of data were collected at 14 receive locations with distances ranging from 0.35 to 1.41 km.

The transmissions from the two cellular base stations at the Naperville and Bellwood sites were identical, and consisted of 5-Watt (EIRP) CW signals radiated by a vertically polarized omnidirectional antenna. The downlink receiver used a dual-polarization antenna with cross slant-45-degree elements and a beamwidth of 30 degrees. The measurements were made at either a test vehicle parked on the street or a tripod placed next to a residence. In all cases, the receiving antenna was pointed in the direction which yielded the strongest downlink signal. (In virtually all cases, this was very close to the direct path to the base.) A commercial narrowband propagation measurement receiver manufactured by Grayson Electronics was used to sample and record the received power on both branches with 1-dB resolution at a fixed rate of 400 samples/second.

2) *The Neighborhoods with Rolling Terrain and Moderate-to-Heavy Foliage:* The New Jersey transmit sites in Whippany and Iselin overlooked a terrain consisting of rolling hills with moderate-to-heavy tree densities and dwellings of one or two stories. A total of 327.5 hours of data were collected at 16 receive locations. In Whippany, 127.5 hours of data were collected at 7 receive locations with distances ranging from 0.49 km to 1.95 km. In Iselin, 200 hours of data were collected at 9 receive locations with distances ranging from 0.84 to 3.11 km.

Each transmitter used a 10-MHz swept frequency source centered at 1985 MHz and a vertically polarized directional transmitting antenna with elevation and azimuth beamwidths of 16° and 65° , respectively. The receiving antenna was the same dual-polarization directional antenna with cross slant- 45° elements that was used in the sites with flat terrain. The receiver was a pair of spectrum analyzers equipped with custom-designed data acquisition software. The measured data consists of power vs. time on each of 100 frequencies spaced at 100 kHz intervals, though only the central 60 frequencies (spanning nearly 6 MHz) were processed.

3) *The Neighborhood with Flat Terrain and Heavy Foliage:* We collected uplink measurements in a suburban neighborhood near the University of British Columbia in Vancouver. The foliage in the area is dense and consists of a mixture of coniferous and deciduous trees. Over 26 hours of data were collected over paths of between 0.46 and 1.41 km in length. All measurement data were collected with the trees in full foliage over a six-week period.

The test vehicle was equipped with a 2-GHz transmitter and a vertically polarized omnidirectional antenna. It radiated 5-Watt (EIRP) CW signals and was driven to 98 randomly

TABLE I

NARROWBAND CHANNEL PARAMETERS SITES WITH FLAT TERRAIN AND LIGHT-TO-MODERATE FOLIAGE

Neighborhood Description					
Transmit Sites	Cellular base stations in Naperville and Bellwood				
Transmit Pol.	Vertical				
Receiving Sites	35 Roadside locations				
Receive Pol.	Cross-slant Linear				
Meas. Span	Time, Location				
Path Lengths	0.35 < d < 2.11 km				
Path Types	Suburban, flat terrain, light to moderately foliated				
Direction	Downlink				
Data Duration	205.5 hours (822 15-minute segments)				
Mean and Standard Deviations					
	\hat{P}_1 (dB)	\hat{P}_2 (dB)	K_1 (dB)	K_2 (dB)	ρ_{env}
μ	0.08	-0.39	16.28	15.80	0.31
σ	1.34	1.17	5.21	4.78	0.25
Correlation Matrix					
	\hat{P}_1 (dB)	\hat{P}_2 (dB)	K_1 (dB)	K_2 (dB)	ρ_{env}
\hat{P}_1 (dB)	1.00	-0.02	0.25	0.04	0.05
\hat{P}_2 (dB)	-0.02	1.00	-0.03	0.14	0.08
K_1 (dB)	0.25	-0.03	1.00	0.89	-0.23
K_2 (dB)	0.04	0.14	0.89	1.00	-0.18
ρ_{env}	0.05	0.08	-0.23	-0.18	1.00

selected locations throughout the area. The receive site was a 25-m tower at the University of British Columbia that was equipped with a dual-polarization antenna with cross-slant elements and a beamwidth of 65°. In all cases, the receiving antenna was pointed in the direction which yielded the strongest uplink signal. (In virtually all cases, this was very close to the direct path to the remote terminal.) An HP8753D vector network analyzer operating in dual-channel tuned-receiver mode was used to sample and record received power on both branches with 0.1 dB resolution at 13 samples/second.

B. Data Reductions

The measurements of path gain vs. time over the two branches were reduced by dividing them into 15-minute segments and estimating the values of the channel parameters for each segment using the methods described in Section II. The segments were initially partitioned into groups by site, the nature of the surrounding terrain, and the distance from the base station. If the statistics of the channel parameters were found to be sufficiently similar, individual sets were combined. Otherwise, they were not.

We have already shown that at any time, location, and frequency, the dual-branch diversity channel can be fully characterized by the five-element state vector, $[P_1, K_1, P_2, K_2, \rho_{env}]$, where P_1 and P_2 are the time-averaged path gains in dB ($P = 10\log G$); and K_1 and K_2 are Ricean K-factors, expressed

TABLE II

NARROWBAND CHANNEL PARAMETERS SITES WITH ROLLING TERRAIN

Neighborhood Description					
Transmit Sites	Towers in Whippany and Iselin				
Transmit Pol.	Vertical				
Receiving Sites	16 Roadside locations				
Receive Pol.	Cross-slant Linear				
Meas. Span	Time, Location, Freq. (6 MHz sub-band)				
Path Lengths	0.49 < d < 3.11 km				
Path Types	Suburban, rolling terrain, light to moderately foliated				
Direction	Downlink				
Data Duration	327.5 hours (1310 15-minute segments)				
Mean and Standard Deviations					
	\hat{P}_1 (dB)	\hat{P}_2 (dB)	K_1 (dB)	K_2 (dB)	ρ_{env}
μ	-0.87	-0.62	8.90	6.02	0.17
σ	3.44	3.08	7.31	7.21	0.22
Correlation Matrix					
	\hat{P}_1 (dB)	\hat{P}_2 (dB)	K_1 (dB)	K_2 (dB)	ρ_{env}
\hat{P}_1 (dB)	1.00	0.27	0.37	0.11	0.10
\hat{P}_2 (dB)	0.27	1.00	-0.06	0.32	0.05
K_1 (dB)	0.37	-0.06	1.00	0.66	-0.21
K_2 (dB)	0.11	0.32	0.66	1.00	-0.22
ρ_{env}	0.10	0.05	-0.21	-0.22	1.00

hereafter in dB. We can remove the range dependence of the average path gains by replacing P_1 and P_2 by $\hat{P}_1 = P_1 - P_g$ and $\hat{P}_2 = P_2 - P_g$, where P_g is either: (1) the dB value of the linear average of the average path gain at a given location, taken over time, frequency, and the two branches; or (2) estimated for a given location using a broadband path gain model, e.g., [9]. Here, we estimated P_g by the first method. Normalizing the average path gains in this manner permits results from different ranges and locations to be directly compared and combined within a single database.

C. Statistics of the Marginal Distributions

In all the cases that we studied, we have found that Gaussian distributions can be used to model the statistics of: (1) the dB values of the average path gains on both branches (and the differences between them), (2) the dB values of the corresponding Ricean K-factors, and (3) the diversity correlation coefficient, ρ_{env} , between branches. We have found that this approximation applies to both: (1) polarization diversity (cross-slant elements) on both the uplink and downlink; and (2) although not reported in detail here, space diversity (linear vertical elements with 10-wavelength separation) on the uplink.

Sample results are shown in Figs. 2 through 6, which give the cumulative distribution functions (CDFs) for \hat{P}_1 , \hat{P}_2 , K_1 , K_2 , and ρ_{env} that were obtained from the uplink

TABLE III
NARROWBAND CHANNEL PARAMETERS SITES WITH FLAT TERRAIN AND
HEAVY FOLIAGE

Neighborhood Description					
Transmit Sites	Roadside vehicle				
Transmit Pol.	Vertical				
Receiving Sites	A base station at UBC				
Receive Pol.	Cross-slant Linear				
Meas. Span	Time, Location				
Path Lengths	0.46 < d < 1.41 km				
Path Types	Suburban, flat terrain, heavily foliated				
Direction	Uplink				
Data Duration	24.5 hours (98 15-minute segments)				
Mean and Standard Deviations					
	\hat{P}_1 (dB)	\hat{P}_2 (dB)	K_1 (dB)	K_2 (dB)	ρ_{env}
μ	-2.01	-1.65	2.64	1.81	0.31
σ	1.81	1.69	5.89	6.10	0.24
Correlation Matrix					
	\hat{P}_1 (dB)	\hat{P}_2 (dB)	K_1 (dB)	K_2 (dB)	ρ_{env}
\hat{P}_1 (dB)	1.00	-0.64	0.67	0.21	0.14
\hat{P}_2 (dB)	-0.64	1.00	0.03	0.48	0.36
K_1 (dB)	0.67	0.03	1.00	0.75	0.53
K_2 (dB)	0.21	0.48	0.75	1.00	0.68
ρ_{env}	0.14	0.36	0.53	0.68	1.00

polarization diversity data collected in the neighborhoods with flat terrain and heavy foliage. The warping of the probability scale is such that a straight line implies a Gaussian distribution. Application of the Anderson-Darling test to these data based on the procedure described in [10] showed that all follow a normal distribution at a 5% significance level. Similar results were obtained for the downlink data from the other neighborhoods. Deviations of the marginal distributions of the model parameters from the Gaussian approximation are most apparent in the tails. For the average path gain distributions, the Gaussian approximation tends to yield slightly conservative estimates. Consideration of the impact of very high and very low values of Ricean K-factor and correlation coefficient suggests that system performance will be relatively insensitive to small departures of the tails from the Gaussian approximation. However, detailed analysis of the sensitivity of a given signaling scheme to such deviations is a topic for future study.

D. Asymmetry between the Polarization Diversity Branches

In our reductions, we often observed significant differences between the average received power and the Ricean K-factors on the two polarization diversity branches. If the polarization of the fixed component of the signal observed at the receiver is vertical, as it will likely be under near LOS conditions with no significant specularly reflected component, the polarization state distribution of the fading signal observed at the receiver

will be centered about vertical polarization and the average received powers and Ricean K-factors observed on the two branches will be equal. If, however, the polarization state of the fixed component is transformed by reflection or diffraction, as may occur under NLOS conditions, or the vertically polarized transmitting antenna and the cross-polarized receiving antenna are rotated with respect to each other, the polarization state distribution observed at the receiver will be offset from the vertical polarization state. In such cases, both the average received power and Ricean K-factor observed on one branch will increase at the expense of those on the other.

IV. THE STATE VECTOR MODEL

In the previous section, we showed that all five elements of the channel state vector can be reasonably modeled as Gaussian random variables over time, place, and frequency. Once again, this result applies to all the data sets we have analyzed, including data measured in both flat and rolling terrain for both uplink and downlink transmission and for both spatial and polarization diversity reception. The implication of this outcome is that we can cast the five elements as a set of jointly Gaussian random variables which can be described by their means, standard deviations, and mutual correlation coefficients or, more concisely, by their mean vector and covariance matrix.

A. Numerical Results

1) *Tabulated Data Reductions*: Channel parameter statistics obtained from reduction of the polarization diversity data from the sites with flat and rolling terrain are presented in Tables I-III. In each case, the mean and standard deviation of each parameter and the correlation matrix are given. Because our estimates of the mean and standard deviation of each distribution are based on channel parameters from hundreds of locations, their statistical reliability is generally high and the corresponding confidence intervals are typically within a few percent of the estimate. The estimates of the correlation matrix are less robust as we discuss below. In the neighborhoods with rolling terrain and moderate-to-heavy foliage, we observe lower average K-factors than we observe in the neighborhoods with flat terrain and light-to-moderate foliage. We also observe higher standard deviations in the neighborhoods with rolling terrain for the path gains and K-factors. These differences are not large, and we attribute them to a terrain differences. We performed statistical analyses on individual frequencies in the sites with rolling terrain, to emulate the data reductions in the sites with flat terrain, and we conclude that the main differences between Tables II and III are more due to the environment than to the number of frequencies measured.

The observed differences notwithstanding, the numerical results are remarkably consistent between the regions. This consistency is especially impressive considering that the corresponding databases were collected by different teams using very different equipment. Thus, it seems likely that the results are accurate and broadly applicable.

2) *Correlation Matrices*: We can further illustrate data consistency by examining and comparing the correlation matrices of Tables I-III. For each matrix, all diagonal values are 1,

TABLE IV
SUMMARY OF CORRELATION COEFFICIENTS (95% CONFIDENCE INTERVAL)

Correlation Coefficient	Downlink (Flat terrain, Light foliage)	Downlink (Rolling terrain, Heavy foliage)	Uplink (Flat terrain, Heavy foliage)
$c(\hat{P}_1, \hat{P}_2)$	$-0.10 < c < 0.05$	$0.22 < c < 0.32$	$-0.75 < c < -0.51$
$c(K_1, K_2)$	$0.88 < c < 0.91$	$0.63 < c < 0.69$	$0.65 < c < 0.85$
$c(\hat{P}_i, K_i), i = 1, 2$	$0.13 < c < 0.26$	$0.29 < c < 0.41$	$0.43 < c < 0.70$
$c(\hat{P}_i, K_j), i \neq j$	$-0.07 < c < 0.07$	$-0.03 < c < 0.08$	$-0.08 < c < 0.31$
$c(\hat{P}_i, \rho_{env}), i = 1, 2$	$0.02 < c < 0.14$	$0.02 < c < 0.13$	$0.05 < c < 0.43$
$c(K_1, \rho_{env}), i = 1, 2$	$-0.26 < c < -0.13$	$-0.27 < c < -0.16$	$0.46 < c < 0.72$

and the values above and below the diagonal have the usual joint symmetry. Thus, the correlation matrix is defined by at most ten independent quantities. The actual number is six, however, because symmetries between the two branches lead to the following equalities: $c(\hat{P}_1, K_1) = c(\hat{P}_2, K_2)$, $c(\hat{P}_1, K_2) = c(\hat{P}_2, K_1)$, $c(\hat{P}_1, \rho_{env}) = c(\hat{P}_2, \rho_{env})$, and $c(K_1, \rho_{env}) = c(K_2, \rho_{env})$, where $c(x, y)$ is the correlation coefficient between x and y . In all three tables, these equalities are satisfied within the statistical accuracy of the data. For each table, therefore, we estimated the six values of c by replacing $c(\hat{P}_1, K_1)$ and $c(\hat{P}_2, K_2)$ with their average, and similarly for the other paired correlations. In addition, we computed the 95% confidence interval for the c -values based upon the assumption that each of the 15-minute segments that we collected at a given time or location was independent of any other. Because the sampling distribution of c is not normally distributed, we converted it to Fisher's z' and computed the confidence interval, then converted the results back to c -values, as described in [11]. The results are given in Table IV.

The downlink results for the sites with flat and rolling terrain (second and third columns) show very strong similarities. The major exception is $c(\hat{P}_1, \hat{P}_2)$. We explain this difference with the following simple analysis: Consider a single location, with data collected over many time segments (as in the sites with flat terrain) or over many narrowband time segments (as in the sites with rolling terrain). For any given time-segment, we can write \hat{P}_1 and \hat{P}_2 as

$$\hat{P}_1 = \Delta P + \delta P \quad (17)$$

$$\hat{P}_2 = \Delta P - \delta P \quad (18)$$

where ΔP is the average of \hat{P}_1 and \hat{P}_2 in that segment (a measure of departure from P_g) and δP is half their difference (a measure of the separation between branches). Both ΔP and δP vary from segment to segment. The correlations between \hat{P}_1 and \hat{P}_2 at the given location is

$$c(\hat{P}_1, \hat{P}_2) = \frac{\text{var}(\Delta P) - \text{var}(\delta P)}{\text{var}(\Delta P) + \text{var}(\delta P)}, \quad (19)$$

where $\text{var}(\cdot)$ is the variance of the argument over all segments. If we define r to be the ratio of the standard deviations of ΔP and δP , then we can recast (19) as

$$c(\hat{P}_1, \hat{P}_2) = \frac{r^2 - 1}{r^2 + 1}. \quad (20)$$

Thus, a slight change in r can produce a noticeable change in $c(\hat{P}_1, \hat{P}_2)$. On the downlinks for the sites overlooking flat

terrain, the variability of the branch gain *differences* was roughly that of the branch gain averages ($r \cong 1.0$) and so $c(\hat{P}_1, \hat{P}_2)$ was near zero. In the sites with rolling terrain, the added variability of ΔP relative to that of δP was small, *i.e.*, r increased from around 1.0 to around 1.29, which was enough to raise $c(\hat{P}_1, \hat{P}_2)$ to 0.25.

We can predict or explain most of the observed trends in the correlation between the remaining parameters using physical intuition and symmetry arguments. For example, when average path gains are uncorrelated between diversity branches, symmetry arguments suggest that the correlation between average path gain and the Ricean K-factor on the opposite branch, and between average path gain and the complex envelope correlation coefficient, should be very low. Results from our database confirm this prediction.

We have also observed similarities between results for single paths and results obtained over many paths and/or frequencies. For example, we have found that Ricean K-factors are generally well-correlated ($\rho > 0.7$) between diversity branches while average path gain and Ricean K-factors on a given branch are only weakly correlated ($\rho \cong 0.3$). We suspect that the weak anti-correlation ($\rho < -0.3$) observed between the complex envelope correlation coefficient and the mean Ricean K-factors on each branch may simply be an artifact of the conservative method used to estimate the complex envelope correlation coefficient from amplitude-only data.

3) *Summary:* We can summarize the numerical results for dual-diversity downlink channels as follows:

- 1) The means of \hat{P}_1 and \hat{P}_2 are close to zero in all cases and should be so approximated in any modeling.
- 2) There is essential equality between the standard deviations of \hat{P}_1 and \hat{P}_2 , those of K_1 and K_2 , and the means of K_1 and K_2 . An exception is the means of K_1 and K_2 on the sites with rolling terrain downlinks, where the difference is larger than expected. The value shown for K_1 (8.9 dB) is very consistent with results from a separate experiment, as reported in [12], and should be used for both branches.
- 3) The K-factor means are several dB higher in sites with flat terrain than in sites with rolling terrain and/or heavy foliage. Also, we know from [12] that the mean is a simple function of distance, season, antenna height, and antenna beamwidth. The numbers given here correspond to a distance of about 1 km, summer, a height of 3 m, and an antenna beamwidth of 30°.
- 4) For flat terrains with light-to-moderate tree densities,

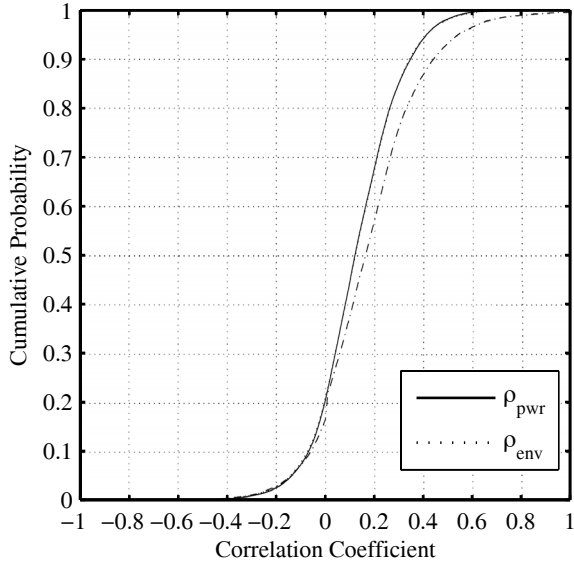


Fig. 1. CDFs for ρ_{pwr} and the worst case estimate of ρ_{env} observed at the sites with rolling terrain.

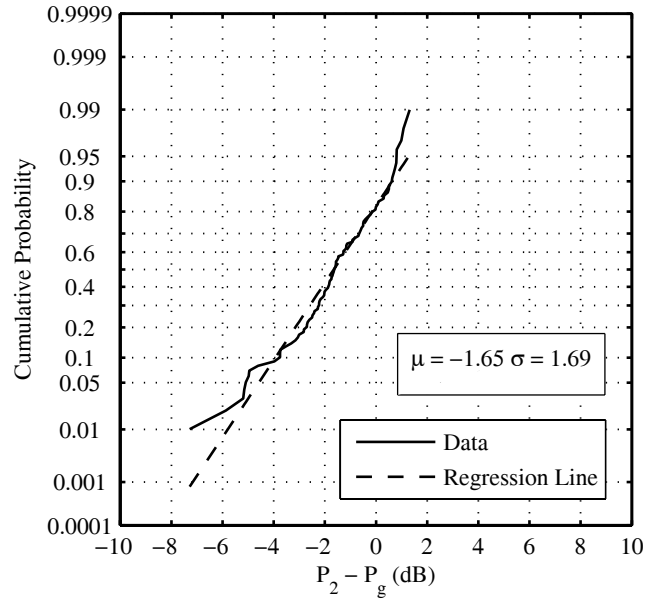


Fig. 3. CDF for uplink $P_2 - P_g$ observed at the sites with flat terrain and heavy foliage (probability scale).

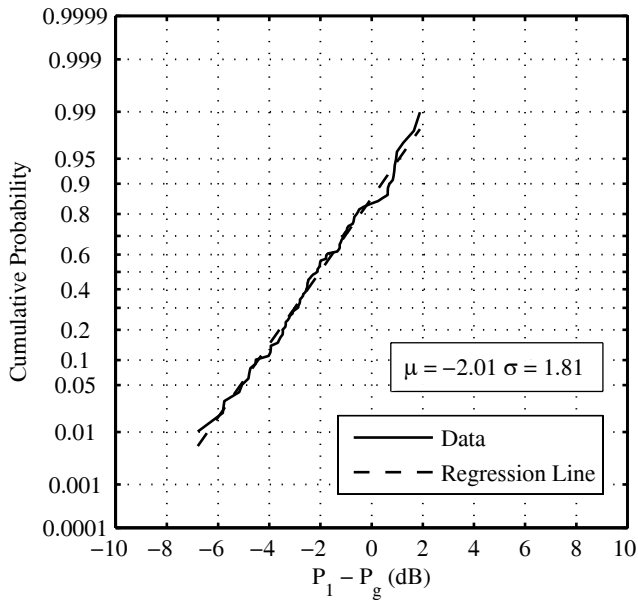


Fig. 2. CDF for uplink $P_1 - P_g$ observed at the sites with flat terrain and heavy foliage (probability scale).

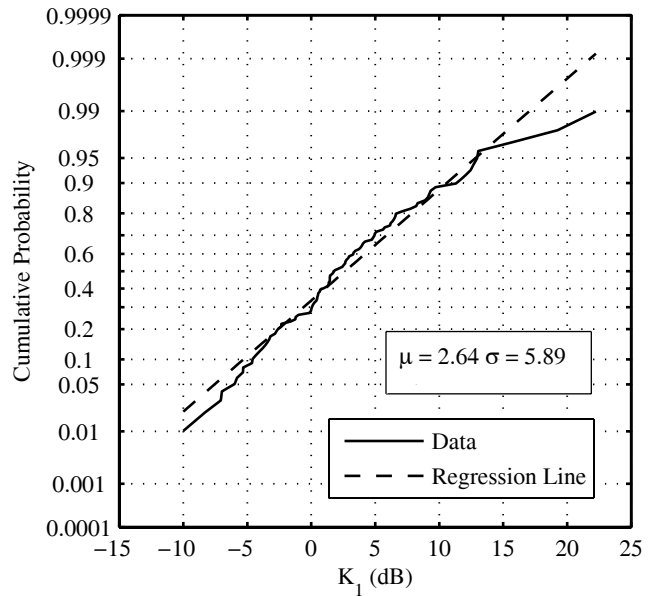


Fig. 4. CDF for uplink K_1 observed at the sites with flat terrain and heavy foliage (probability scale).

means and standard deviations like those in Table I, combined with c-values in the first column of Table IV, would be appropriate. The means and standard deviations in Table II, modified as suggested above and combined with the c-values in the middle column of Table IV, are the model parameters to use in simulating hilly, tree-laden environments. For flat terrain with heavy tree densities, means and standard deviations like those in Table III, combined with c-values in the last column of Table IV, would be more appropriate.

B. Applications

For simulation studies, it is necessary to generate a random sequence of channel state vectors \mathbf{D}' which has the same first order statistics as the measured propagation data. Since the five elements of the channel state vector can be cast as a set of jointly Gaussian random variables described by a mean vector $\boldsymbol{\mu}$ and covariance matrix $[C]$, this can be done in a simple and accurate way. If \mathbf{U} is a sequence of i.i.d. Gaussian r.v.'s with zero mean and unit variance, the random sequence \mathbf{D}' can be

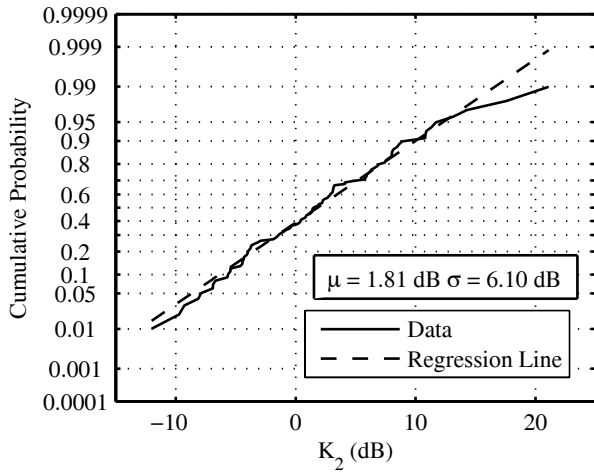


Fig. 5. CDF for uplink K_2 observed at the sites with flat terrain and heavy foliage (probability scale).

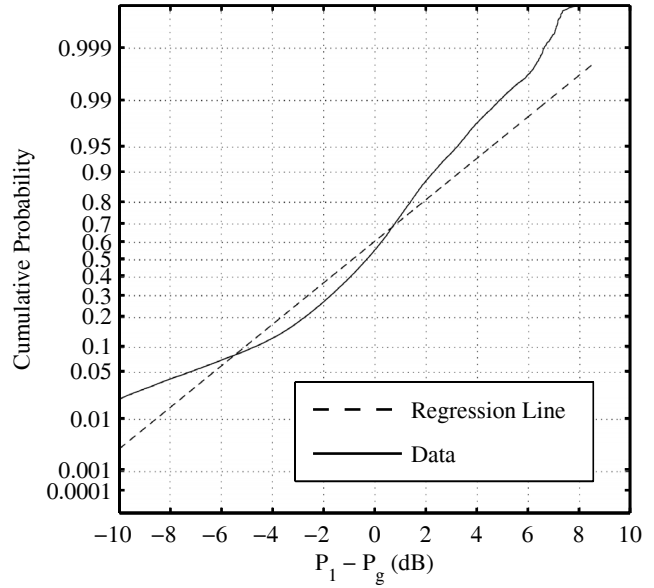


Fig. 7. CDF for downlink $P_1 - P_g$ observed at the sites with rolling terrain (probability scale).

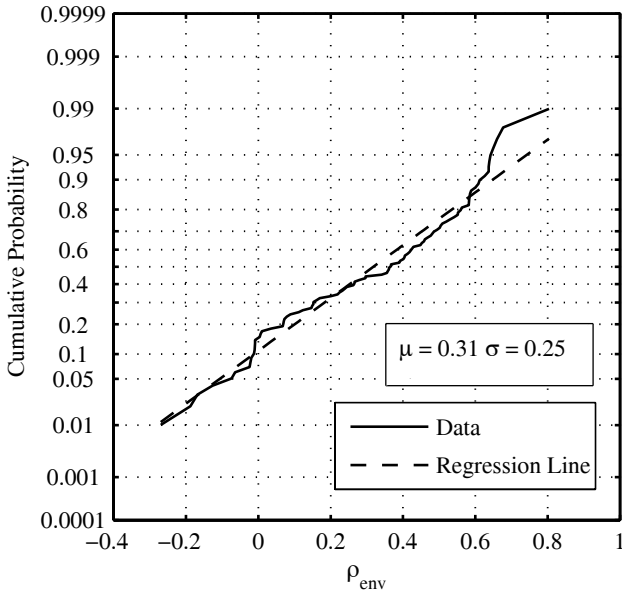


Fig. 6. CDF for uplink ρ_{env} observed at the sites with flat terrain and heavy foliage (probability scale).

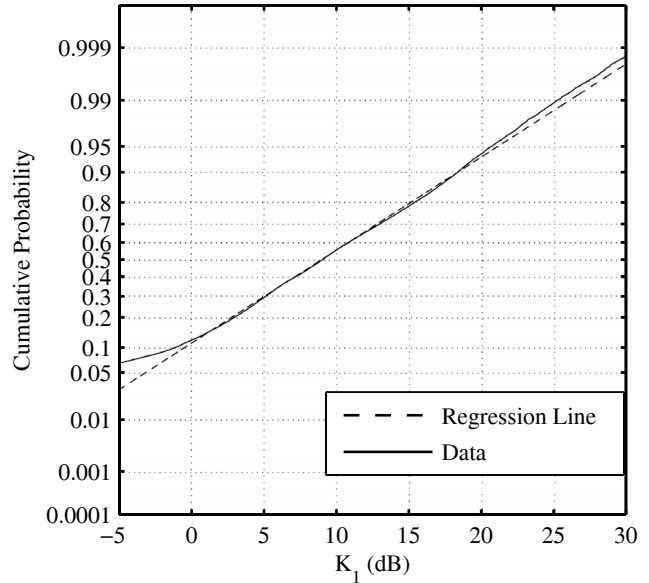


Fig. 8. CDF for downlink K_1 observed at the sites with rolling terrain (probability scale).

obtained by the transformation,

$$\mathbf{D}' = \mathbf{U}\text{chol}[\mathbf{C}] + \boldsymbol{\mu} \tag{21}$$

where $\text{chol}[\mathbf{C}]$ is the upper triangular Cholesky factorization of the covariance matrix.

It is sometimes necessary to model the first order statistics of n -branch ($n > 2$) diversity reception involving spatial, polarization, angular, or frequency diversity or combinations of them, *e.g.*, [13]. It seems likely that our Gaussian random process model for the spatial and polarization diversity channel state vectors applies to angular and frequency diversity, as well. In the general case, ρ are the $n(n-1)/2$ upper (or lower) off-diagonal elements of the matrix of complex envelope correlation coefficients between the time-varying parts of the n path gains. Thus, in general, $n(n+3)/2$ channel parameters

are required to model n -branch diversity.

We have proposed this model specifically for the case of terrestrial fixed wireless systems operating in macrocell propagation environments. However, this modeling approach could prove useful in other cases where fading is Ricean-distributed, such as earth-space communication links. Determination of whether the parameters can also be modeled as jointly Gaussian random processes would require collection and analysis of a propagation database in a manner similar to that undertaken here for the terrestrial case.

V. CONCLUSIONS

We have shown that the first-order statistics of two-branch diversity reception over narrowband fixed wireless Ricean channels is completely described by just five channel parameters: the average path gains and Ricean K-factors for each branch and the complex envelope correlation coefficient between the time-varying components of the two path gains. All five parameters can be estimated from amplitude-only measurements of path gain vs. time, subject only to the assumption that the time-varying component of the path gain is complex Gaussian. The model can easily be generalized to narrowband diversity reception with multiple branches.

Our analysis of the propagation data that we collected in typical suburban macrocell environments supports representing the set by a five-element vector of jointly random Gaussian variates. Moreover, the form of the parameter correlation matrix can be deduced using a combination of physical insight and symmetry arguments. Despite obvious differences between the neighborhoods in which the data was collected, the results obtained show a remarkable consistency and it is likely that they are broadly applicable.

ACKNOWLEDGEMENTS

We are indebted to numerous past and present AT&T colleagues and contractors for collecting and processing the large quantities of data used in this study. They are D. J. Barnickel, M. K. Dennison, B. J. Guarino, P. B. Guerlain, D. Jacobs, S. C. Kim, R. S. Roman, A. J. Rustako, Jr., S. K. Wang, J. Lee, L. Roberts and M. Stephano. Thanks also to Anthony Liou of the University of British Columbia for his considerable assistance with the collection and processing of the data from the Vancouver site. We are also indebted to Andreas F. Molisch for his valuable advice on improving this paper.

REFERENCES

- [1] V. Erceg, D. G. Michelson, S. S. Ghassemzadeh, L. J. Greenstein, A. J. Rustako, Jr., P. B. Guerlain, M. K. Dennison, R. S. Roman, D. J. Barnickel, S. C. Wang, and R. R. Miller, "A model for the multipath delay profile of fixed wireless channels," *IEEE J. Select. Areas Commun.*, vol. 17, no. 3, pp. 399-410, Mar. 1999.
- [2] M. J. Gans, N. Amitay, Y. S. Yeh, T. C. Damen, R. A. Valenzuela, C. Cheon, and J. Lee, "Propagation measurements for fixed wireless loops (FWL) in a suburban region with foliage and terrain blockages," *IEEE Trans. Wireless Commun.*, vol. 1, no. 2, pp. 302-310, Apr. 2002.
- [3] V. Erceg, P. Soma, D. S. Baum, and S. Catreux, "Multiple-input multiple-output fixed wireless radio channel measurements and modeling using dual-polarized antennas at 2.5 GHz," *IEEE Trans. Wireless Commun.*, vol. 3, no. 6, pp. 2288-2298, Nov. 2004.
- [4] L. Ahumada, R. Feick, and R. A. Valenzuela, "Characterization of temporal fading in urban fixed wireless links," *IEEE Commun. Lett.*, vol. 10, no. 4, pp. 242-244, Apr. 2006.
- [5] L. J. Greenstein, V. Erceg, and D. G. Michelson, "Modeling diversity reception over narrowband fixed wireless channels," *Electron. Lett.*, vol. 34, no. 11, pp. 1146-1147, 28 May 1998.
- [6] D. G. Michelson, V. Erceg, and L. J. Greenstein, "Modeling diversity reception over narrowband fixed wireless channels," *IEEE MTT-S Symposium on Technologies for Wireless Applications*, Feb. 1999, pp. 95100.
- [7] D. Greenwood and L. Hanzo, "Characterisation of mobile radio channels," in *Mobile Radio Communications*, R. Steele, ed. London: Pentech Press, 1992, pp. 163-177.
- [8] L. J. Greenstein, D. G. Michelson, and V. Erceg, "Moment-method estimation of the Ricean K-Factor," *IEEE Commun. Lett.*, vol. 3, no. 6, pp. 175-176, June 1999.

- [9] V. Erceg, L. J. Greenstein, S. Y. Tjandra, S. R. Parkoff, A. Gupta, B. Kulic, A. A. Julius, and R. Bianchi, "An empirically based path loss model for wireless channels in suburban environments," *IEEE J. Select. Areas Commun.*, vol. 17, no. 7, pp. 1205-1211, July 1999.
- [10] M. A. Stephens, "EDF statistics for goodness of fit and some comparisons," *J. Amer. Statistical Assoc.*, vol. 69, no. 347, pp. 730-737, Sept. 1974.
- [11] M. G. Bulmer, *Principles of Statistics*, 2nd ed. Edinburgh, UK: Oliver and Boyd, 1967, pp. 209-230.
- [12] L. J. Greenstein, S. S. Ghassemzadeh, V. Erceg, and D. G. Michelson, "Ricean K-factors in narrowband fixed wireless channels," *IEEE Trans. Veh. Technol.*, in press.
- [13] J. H. Winters, "Smart antennas for wireless systems," *IEEE Personal Commun.*, vol. 5, no. 1, pp. 23-27, Feb. 1998.



David G. Michelson (S'80-M'89-SM'99) received the B.A.Sc., M.A.Sc., and Ph.D. degrees in electrical engineering from the University of British Columbia (UBC), Vancouver, BC, Canada.

From 1996 to 2001, he served as a member of a joint team from AT&T Wireless Services, Redmond, WA, and AT&T LabsResearch, Red Bank, NJ, where he was concerned with the development of propagation and channel models for next-generation and fixed wireless systems. The results of this work formed the basis for the propagation and channel

models later adopted by the IEEE 802.16 Working Group on Broadband Fixed Wireless Access Standards. From 2001 to 2002, he helped to oversee the deployment of one of the worlds largest campus wireless local area networks at UBC while also serving as an Adjunct Professor with the Department of Electrical and Computer Engineering. Since 2003, he has led the Radio Science Laboratory, Department of Electrical and Computer Engineering, UBC, where his current research interests include propagation and channel modeling for fixed wireless, ultra wideband, and satellite communications.

Prof. Michelson is a registered professional engineer. He serves as the Chair of the IEEE Vehicular Technology Society Technical Committee on Propagation and Channel Modeling and as an Associate Editor for Mobile Channels for IEEE VEHICULAR TECHNOLOGY MAGAZINE. In 2002, he served as a Guest Editor for a pair of Special Issues of the IEEE JOURNAL ON SELECTED AREAS IN COMMUNICATIONS concerning propagation and channel modeling. From 2001 to 2007, he served as an Associate Editor for the IEEE TRANSACTIONS ON VEHICULAR TECHNOLOGY. From 1999 to 2007, he was the Chair of the IEEE Vancouver Sections Joint Communications Chapter. Under his leadership, the chapter received Outstanding Achievement Awards from the IEEE Communications Society in 2002 and 2005 and the Chapter of the Year Award from IEEE Vehicular Technology Society in 2006. He received the E. F. Glass Award from IEEE Canada in 2009 and is currently the Chair of IEEE Vancouver Section.

Vinko Erceg (M'92-SM'98-F'07) received the B.Sc. degree in electrical engineering and the Ph.D. degree in electrical engineering from the City University of New York, in 1988 and 1992, respectively.



From 1990 to 1992, he was a Lecturer with the Department of Electrical Engineering, City College of the City University of New York. Concurrently, he was a Research Scientist with SCS Mobilecom, Port Washington, NY, working on spread-spectrum systems for mobile communications. In 1992, he joined AT&T Bell Laboratories. In 1996, he joined AT&T LabsResearch as a Principal Member of Technical Staff with the Wireless Communications Research Department, where he worked on signal propagation and other projects related to the systems engineering and performance analysis of personal and mobile communication systems. From 2000 to 2002, he was with Iospan Wireless Inc., San Jose, CA, as the Director of the Communication Systems Division, working on system, propagation, deployment, and performance issues of a multiple-input-multiple-output orthogonal frequency division multiplexing communication system. He is currently a Senior Manager with the Broadcom Corp., San Diego, CA.



Saeed S. Ghassemzadeh (S'88-M'91-SM'02) received the B.S., M.S., and Ph.D. degrees in electrical engineering from the City University of New York, New York, in 1989, 1991, and 1994, respectively.

From 1989 to 1992, he was with SCS Mobilecom, which is a wireless technology development company, where he conducted research in the areas of wireless channel modeling. In 1992, while working toward the Ph.D. degree, he joined InterDigital, where he worked as a Principal Research Engineer, conducting research in the areas of fixed/mobile

wireless channels, and was involved in system integration and testing of B-code-division multiple access (CDMA) technology. At the same time, he was also an Adjunct Lecturer at the City University of New York. In 1995, he joined AT&T Wireless Communication Center of Excellence, AT&T Bell Laboratories, where he was involved in the design and development of the fixed wireless base station. He also conducted research in areas of CDMA technologies, propagation channel measurement and modeling, satellite communications, wireless local area networks, and coding in wireless systems. He is currently Principal Member of Technical Staff with the Communication Technology Research Department at AT&T Labs-Research, Florham Park, NJ. His current research interest includes wireless propagation measurement and modeling, cognitive radio, wireless local area networks, and terahertz communications.

Dr. Ghassemzadeh is a member of the IEEE Communication Society and IEEE Vehicular Technology Society. He is currently an Associate Editor for the IEEE TRANSACTIONS ON WIRELESS COMMUNICATIONS and the JOURNAL OF COMMUNICATIONS AND NETWORKS.



Larry J. Greenstein (S'59-M'67-SM'80-F'87-LF'02) received the B.S., M.S., and Ph.D. degrees in electrical engineering from the Illinois Institute of Technology, Chicago, in 1958, 1961, and 1967, respectively.

From 1958 to 1970, he was with IIT Research Institute, Chicago, working on radio frequency interference and anticlutter airborne radar. He joined Bell Laboratories, Holmdel, NJ, in 1970. He was with AT&T for 32 years, conducting research on digital satellites, point-to-point digital radio, optical transmission techniques, and wireless communications. For 21 years during that period (1979-2000), he led a research department renowned for its contributions in these fields. He is currently a Research Scientist with the Wireless Information Network Laboratory (WINLAB), Rutgers University, North Brunswick, NJ, working in the areas of ultrawideband, sensor networks, multiple-input-multiple-output-based systems, broadband power line systems, and radio channel modeling. He has been a Guest Editor, Senior Editor, and Editorial Board Member for numerous publications.

Dr. Greenstein is an AT&T Fellow. He is a recipient of the IEEE Communications Society's Edwin Howard Armstrong Award and a corecipient of four best paper awards. He is currently the Director of Journals for the IEEE Communications Society.